

ORIGINAL ARTICLE

Chromosomal imbalances and partial uniparental disomies in primary central nervous system lymphoma

H Schwindt^{1,5}, I Vater^{2,5}, M Kreuz³, M Montesinos-Rongen¹, A Brunn¹, J Richter², S Gesk², O Ammerpohl², OD Wiestler⁴, D Hasenclever³, M Deckert^{1,6} and R Siebert^{2,6}

¹Department of Neuropathology, University Hospital of Cologne, Cologne, Germany; ²Institute of Human Genetics, Christian-Albrechts-University Kiel, University Hospital Schleswig-Holstein, Campus Kiel, Kiel, Germany; ³Institute for Medical Informatics, Statistics and Epidemiology, (IMISE), University of Leipzig, Leipzig, Germany and ⁴German Cancer Research Center, Heidelberg, Germany

To determine the pattern of genetic alterations in primary central nervous system lymphomas (PCNSL), 19 PCNSL were studied by high-density single-nucleotide polymorphism arrays. Recurrent losses involved 6p21.32, 6q21, 8q12–12.2, 9p21.3, 3p14.2, 4q35.2, 10q23.21 and 12p13.2, whereas gains involved 18q21–23, 19q13.31, 19q13.43 and the entire chromosomes X and 12. Partial uniparental disomies (pUPDs) were identified in 6p and 9p21.3. These genomic alterations affected the HLA locus, the *CDKN2A/p16*, *CDKN2B/p15* and *MTAP*, as well as the *PRDM1*, *FAS*, *MALT1*, and *BCL2* genes. Increased methylation values of the *CDKN2A/p16* promoter region were detected in 75% (6/8) PCNSL. Gene expression profiling showed 4/21 (20%) minimal common regions of imbalances to be associated with a differential mRNA expression affecting the *FAS*, *STAT6*, *CD27*, *ARHGEF6* and *SEPT6* genes. Collectively, this study unraveled novel genomic imbalances and pUPD with a high resolution in PCNSL and identified target genes of potential relevance in the pathogenesis of this lymphoma entity.

Leukemia (2009) 23, 1875–1884; doi:10.1038/leu.2009.120;
published online 4 June 2009

Keywords: primary CNS lymphoma; genetics; SNP array

Introduction

Primary central nervous system lymphomas (PCNSL) are aggressive B-cell lymphomas confined to the central nervous system associated with a poor prognosis.^{1,2} They are classified as diffuse large B-cell lymphoma (DLBCL).^{3,4} However, it is still a matter of debate whether they differ from systemic DLBCL with respect to their molecular features and pathogenesis.

Studies addressing the genetic characteristics of PCNSL identified recurrent chromosomal abnormalities.^{5–7} In addition to translocations of the immunoglobulin (*IG*) and the *BCL6* loci present in a subset of PCNSL, gains and losses of genetic material are recurrent in PCNSL.^{8,9} Gains of 18q were the most frequent alteration (38%) in one series of 13 PCNSL analyzed by interphase fluorescence *in situ* hybridization (FISH).⁵ High-level amplifications were mapped to 18q21–23 by comparative genomic hybridization to chromosomes in two tumors of a series of 19 PCNSL.⁷ In addition, gains of 12q (63%, 12/19), 1q, 9q, 16p, and 17q (26% each, 5/19) were identified by comparative genomic

hybridization and/or FISH.⁷ Furthermore, deletion of 6q was reported in 47% (9/19) PCNSL.⁷ Finally, deletion of the human leukocyte antigen (HLA) class II region in 6p21.32 including homozygous loss was reported to affect more than half of all PCNSL and to be associated with loss of MHC expression.^{10–12}

Although these studies provided interesting and important insights into the genetic abnormalities in PCNSL, they were limited by a low resolution and the inability to detect partial uniparental disomy (pUPD). Therefore, a series of 19 PCNSL was studied by high-density single-nucleotide polymorphism (SNP) arrays. This high-resolution technology allowed narrowing down chromosomal regions of interest and, furthermore, identification of novel imbalances and regions with pUPD.

Materials and methods

Clinical data

Stereotactic biopsies of 19 immunocompetent patients (11 females and 8 males) were included in this study. All studies were approved by local ethics committees. Informed consent was provided according to the Declaration of Helsinki Principles. Systemic lymphoma manifestation was excluded by extensive staging. All PCNSL were histopathologically classified as CD20+ DLBCL according to the World Health Organization (WHO) classification.³ The diagnoses were based on a combination of routine morphology and immunohistochemistry using monoclonal mouse antibodies against CD20, CD45, Ki-67 (MIB-1), IgM, IgG, BCL6, and MUM1/IRF4 as reported earlier.^{13,14} The clinical characteristics are summarized in Table 1.

GeneChip 100k mapping array

DNA extraction was carried out as reported previously.¹⁵ For each tumor sample, a total of 500 ng DNA were processed according to the Affymetrix GeneChip Mapping 100k Assay Manual (Affymetrix, Santa Clara, CA, USA). Briefly, 250 ng of genomic DNA was digested with *Xba*I or *Hind*III and ligated to GeneChip Human Mapping 50k adaptors. Adaptor-ligated restriction fragments were amplified by PCR, purified, fragmented and labeled as described.¹⁶ Samples were hybridized to GeneChip Human Mapping 50k *Xba*240 or *Hind*240 arrays (Affymetrix) using the Affymetrix Hybridization Oven 640 (Affymetrix). Washes and staining of the arrays were performed with an Affymetrix Fluidics Station 450 (Affymetrix), and images were obtained using an Affymetrix GeneChip Scanner 3000 (Affymetrix).

Correspondence: Professor Dr M Deckert, Department of Neuropathology, University Hospital of Cologne, Kerpener Str. 62, Köln D-50924, Germany.

E-mail: martina.deckert@uni-koeln.de

⁵These authors contributed equally to the work.

⁶These authors share senior authorship.

Received 11 March 2009; accepted 27 March 2009; published online 4 June 2009

Table 1 Patients' data

PCNSL no.	Gender	Age at diagnosis	Affected MCRs	DLBCL subtype significance
01	M	81	1, 5, 6, 10, 12, 13, 16, 19, and 20	GCB
02	F	61	5, 9, 14, and 18	GCB
03	F	68	2, 3, 4, 5, 6, 8, 9, 11, 18, and 20	ABC
04	F	67	1, 5, 6, 10, 12, 18, 19, and 20	GCB
05	F	75	3, 5, 6, 7, 12, 19, 20, and 21	ABC
06	M	66	2, 3, 5, 6, 10, 11, 13, 17, 18, 19, and 20	'type 3'
07	F	77	5, 9, 11, 16 and 21	'type 3'
08	F	78	17	'type 3'
09	M	56	—	'type 3'
10	F	75	21	GCB
11	F	65	17 and 20	ABC
12	F	82	6, 11, 14, 18, 19, and 21	'type 3'
13	M	52	1, 2, 4, 5, 11, 15, 16, and 20	'type 3'
14	F	47	5, 11, and 14	GCB
15	F	76	4, 5, 6, 9, 13, 14, 18, 19, 20, and 21	GCB
16	M	68	5, 7, 8, 16 and 18	GCB
17	M	74	2, 3, 4, 5, 6, 7, 8, 9, 11, 13, 15, and 17	ABC
18	M	55	1, 5, 6, 9, 10, 11, 12, 15, 18 and 21	ABC
19	M	54	5, 6, 7, 8, 11, 14, 15, 16, 19, and 20	NA

Abbreviations: ABC, GCB, 'type 3', activated B-cell-like, germinal center B-cell-like and 'type 3' (non-ABC/non-GCB) of DLBCL classified by gene expression profiling; DLBCL, diffuse large B-cell lymphoma; F, female; M, male; MCR, minimal common region, note that only regions with alterations in more than 20% are assigned as described in Table 2; NA, not analyzed; PCNSL, primary central nervous system lymphoma; pUPD, partial uniparental disomy.

Data analysis

Reference samples: As reference, 90 HapMap samples (30 Centre d'Etude du Polymorphisme Humain (CEPH) trios) provided by Affymetrix were used (http://www.affymetrix.com/support/technical/sample_data/hapmap_trio_data.affx). The reference set was completed by a set of seven samples with diploid karyotypes hybridized in the same laboratory as the tumor samples.

Genotyping: The Bayesian robust linear model with Mahalanobis distance classifier (BRLMM) algorithm¹⁷ was used with default parameters (score threshold = 0.5, prior size = 10 000, and dynamic model (DM) threshold = 0.17) to genotype tumor samples together with euploid reference arrays.

Copy number analysis: Copy number was analyzed using the CNAG program v2.0 using the optimized reference selection method implemented in CNAG.¹⁸ Thus, CNAG selected a gender-specific reference set out of the 97 controls individually for each array. *Xba*240 and *Hind*240 arrays were combined for the analysis. Segmentation of raw copy number data was carried out using the Hidden Markov Model (HMM) approach provided by CNAG. HMM parameters were adjusted individually for each array because of the differences in hybridization quality and tumor cell content (at least 80% as assured morphologically). Starting with default parameters, the mean levels of HMM states were manually adjusted to optimize segmentation results for each sample.

With regard to outliers and technical artifacts, HMM segments with aberrant copy number were considered as copy number aberration only if they consisted of at least 10 consecutive SNPs. The given breakpoints refer to the first neighboring SNPs without alteration. Homozygous deletions were defined as aberrations with copy number = 0. Aberrant regions were compared to the published data of the 'Database of Genomic variants.'¹⁹ Regions showing overlap >50% with known genomic variants were classified as copy number polymorphisms (CNV).

Detection of loss of heterozygosity/pUPD: The HMM-based method²⁰ implemented in the dChip program (build date: 11

April 2007)^{21,22} was used to infer regions with loss of heterozygosity (LOH). The HMM considering haplotype (linkage disequilibrium (LD)-HMM)²⁰ method was selected for the LOH calculations to account for LD-induced SNP dependencies. The LOH call threshold was set to the default value of 0.5. An empirical haplotype²⁰ correction was applied. Thus, the genotypes of putative tumor LOH regions were compared with those observed in euploid reference samples. If the genotypes in the respective region were highly concordant between the tumor sample and at least 5% of the normal reference samples, the LOH region was rejected by dChip.

pUPD regions represent genomic regions in which LOH is not caused by altered copy number. LOH regions determined by dChip were called pUPD if copy number analysis using CNAG did not show aberrations within that region. If an LOH region was partially affected by copy number aberrations, subregions with normal copy number were called pUPD if they comprised at least 50 neighboring SNPs.

Correlation of minimal common regions with gene expression profiles

For all PCNSL (i.e., case nos. 1–18), except for PCNSL 19, gene expression profiles were available (GEO database²³ GSE6047²⁴). For all mRNAs in the minimal common regions (MCR) detected by SNP, corresponding tags on the HG-U95Av2 platform (Affymetrix) were evaluated for mRNA expression. Normalized gene expression profiles²⁴ were analyzed in geWorkbench (<http://wiki.c2b2.columbia.edu/workbench/index.php/Home>). After replacing all values below 100 by 100 (background noise correction) and log₂ transformation, mRNAs of tumors harboring these MCRs were compared with those without genetic alterations in these loci as evidenced by SNP analysis. Statistically significant differential expression was determined using Student's *t*-test with α -correction.

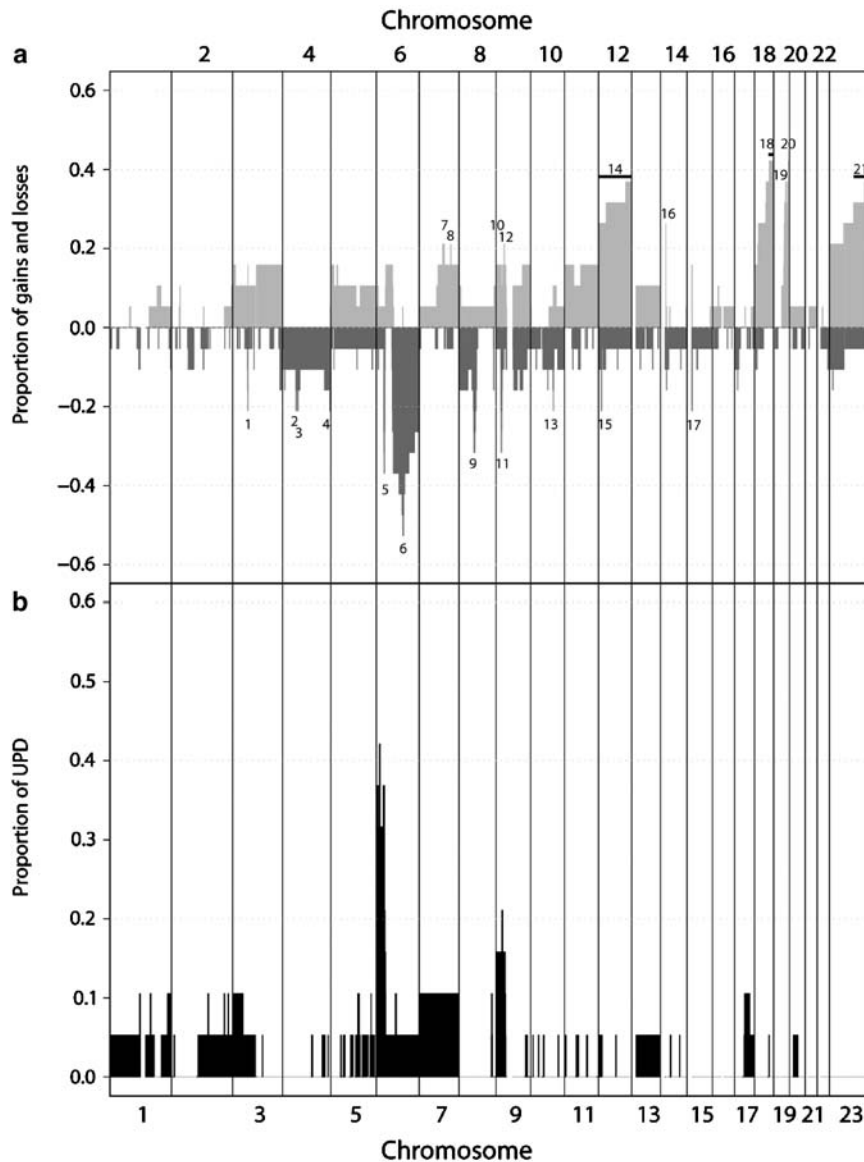


Figure 1 Genome-wide detection of copy number changes and regions with pUPD analyzing 100k GeneChip data of 19 PCNSL. (a) Proportion of gains and losses are displayed from 1pter (left) to Xqter (right). Light gray columns indicate chromosomal gain, whereas dark gray columns indicate loss of genetic material. The numbers indicate MCRs of frequent imbalances described in Table 2. (b) Proportions of pUPD from 1pter (left) to Xqter (right).

Sequencing of the *PRDM1* gene

Sequencing of the *PRDM1* gene was carried out as described previously.²⁵ In brief, all exons of the *PRDM1* gene were amplified by PCR. Amplicons were separated by agarose gel electrophoresis, subsequently cleaned up and directly sequenced from both sides.

FISH

To verify copy number results from 100k GeneChip analyses, dual-color FISH was applied. FISH probes consisted of spectrum orange (so) or spectrum green (sg) (Abbott/Vysis, Downers Grove, IL, USA) labeled P1-derived or bacterial artificial chromosome (PAC/BAC) clones (Invitrogen, Karlsruhe, Germany). The clones RP1-93N13 (so) and RP1-172K2 (sg)¹² were used to detect deletions in the HLA region in 6p21.32, and

clones RP11-140A9 (sg) and RP11-1081N13 (so) to detect deletions in 8q12. In addition, two commercial assays were applied to confirm copy number changes of *MALT1* and *ETV6* (LSI *MALT1* and LSI *ETV6* dual-color break apart probes, Abbott/Vysis). Probe preparation and FISH were performed as published.²⁶ Whenever possible, at least 100 interphase nuclei were evaluated per hybridization.

Bisulfite pyrosequencing

Bisulfite pyrosequencing of *CDKN2A/p16* was performed according to standard protocols with slight modifications in eight PCNSL (case nos. 02, 03, 06, 10, 11, 14, 17 and 19), in which sufficient material was available.²⁷ Briefly, genomic DNA was bisulfite converted using the EpiTect Bisulfite Conversion Kit (Qiagen, Hilden, Germany). In a subsequent PCR amplification, locus-specific primers were used with one primer

Table 2 MCR of frequent imbalances in 19 PCNSL

MCR	Cytoband	Physical mapping (Mb) ^a	Frequency	Candidate genes ^b
1	Loss: 3p14.2	60.7–60.8	4/19 (21%)	<i>FHIT</i>
2	4q12	53.6–54.0	4/19 (21%)	<i>SCFD2</i>
3	4q13.1	60.2–61.0	4/19 (21%)	Unknown
4	4q35.2	187.8–189.3	4/19 (21%)	<i>FAT, ZFP42</i>
5	6p21.32	32.5–32.7	7/19 (37%) 2 HZD, +7 pUPD (7/19; 37%)	<i>HLA-DRB, HLA-DQA, HLA-DQB</i>
6	6q21	106.4–108.4	10 /19 (52%)	<i>PRDM1</i>
9	8q12.1–q12.2	59.8–62.2	6 /19 (32%)	<i>TOX; CA8; RAB2A</i>
11	9p21.3	21.7–22.7	6/19 (32%) 1 HZD+3 pUPD (3/19; 16%)	<i>MTAP, CDKN2A/p16, CDKN2B/p15</i>
13	10q23.21	90.7–90.8	4/19 (21%)	<i>FAS^d, AMSH-LP</i>
15	12p13.2	11.7–11.9	4/19 (21%) 1 HZD	<i>ETV6</i>
17	15q11.2	19.2 ^c –20.6	4/19 (21%)	(CNV)
7	Gain: 7q21.3–q22.1	93.8–100.4	4/19 (21%)	Unknown
8	7q31.33	125.6–125.7	4/19 (21%)	(CNV)
10	9p24.3	0.2 ^c –0.5	4/19 (21%)	(CNV)
12	9p13.3	33.0–34.5	4/19 (21%)	<i>NFX1, BAG1</i>
14	12	Pter-Qter	5/19 (26%)	Several (<i>STAT6, CD27</i>) ^d
16	14q11.2	21.6–22.0	5/19 (26%)	(CNV)
18	18q21.33–q23	58.8 (47.0)–76.1	8/19 (43%)	<i>BCL2, (MALT1)</i>
19	19q13.31	48.2–49.3	7/19 (37%)	<i>ZNF</i> cluster (<i>ETHE1</i>) ^d
20	19q13.43	61.5–63.8	9/19 (47%)	<i>ZNF</i> cluster
21	Xq21.33–q28	95.8–154.8	6/19 (32%)	Unknown (<i>ARHGEF6, SEPT6</i>) ^d

Abbreviations: CNV, copy number variation according to the Database of Genomic Variants; HZD, homozygous deletion; MCR, minimal common region; pUPD, partial uniparental disomy.

^aAccording to NCBI Build 35.

^bCommon genes with typical tumor suppressor or oncogene properties.

^cPosition of first SNP represented on the microarray.

^dDifferentially expressed genes as determined by gene expression profiling.

biotinylated at the 5'-end (5'biotin-GAGGGGTTGGTTGGTTAT TAGA-3'; 5'-CTACAAACCCCTACCCACCTAA-3'). Amplification reactions contained ~75 ng bisulfite-converted DNA, primers, AccuPrime Taq Polymerase and buffer II (Invitrogen, Karlsruhe, Germany), 50 mM MgCl₂ and 5 mM of each dNTP in a final volume of 50 µl. After initial denaturation, PCR consisted of 45 cycles of each 95 °C for 30 s, 60 °C for 30 s and 68 °C for 30 s, followed by a final synthesis at 68 °C for 2 min. PCR products were verified by gel electrophoresis. Single strands were prepared using the VacuumPrep Tool (Biotage, Uppsala, Sweden), followed by a denaturation step at 85 °C for 2 min and final sequencing primer (5'-CCCTCTACCCACCTAAAT-3') hybridization. Pyrosequencing was performed using the Pyrosequencer ID and the DNA methylation analysis software Pyro Q-CpG 1.0.9 (Biotage), which was also used to quantify the ratio T:C (mC:C) at the CpG sites analyzed. Assays were validated using an *in vitro* methylated DNA (Millipore, Billerica, MA, USA) and pooled

DNA was isolated from 20 peripheral blood samples from 10 men and 10 women. The latter was also used as a normal control.

Results

Frequency of genomic imbalances and pUPD

All PCNSL harbored at least three regions of chromosomal imbalances or pUPD. The median of aberrant regions per PCNSL was 18. A genomic overview of gains and losses detected in the 19 investigated PCNSL is presented in Figure 1a. A total of 188 genomic losses (median per PCNSL: 9, range: 0–32) and 126 genomic gains (median per PCNSL: 6, range: 0–13) were identified. Overlapping genomic segments of copy number changes delineated MCRs. In each of the cases, between 0 and 12 MCRs were affected. Chromosomal regions that were affected in at least 4 (21%) PCNSL are summarized in Table 2.

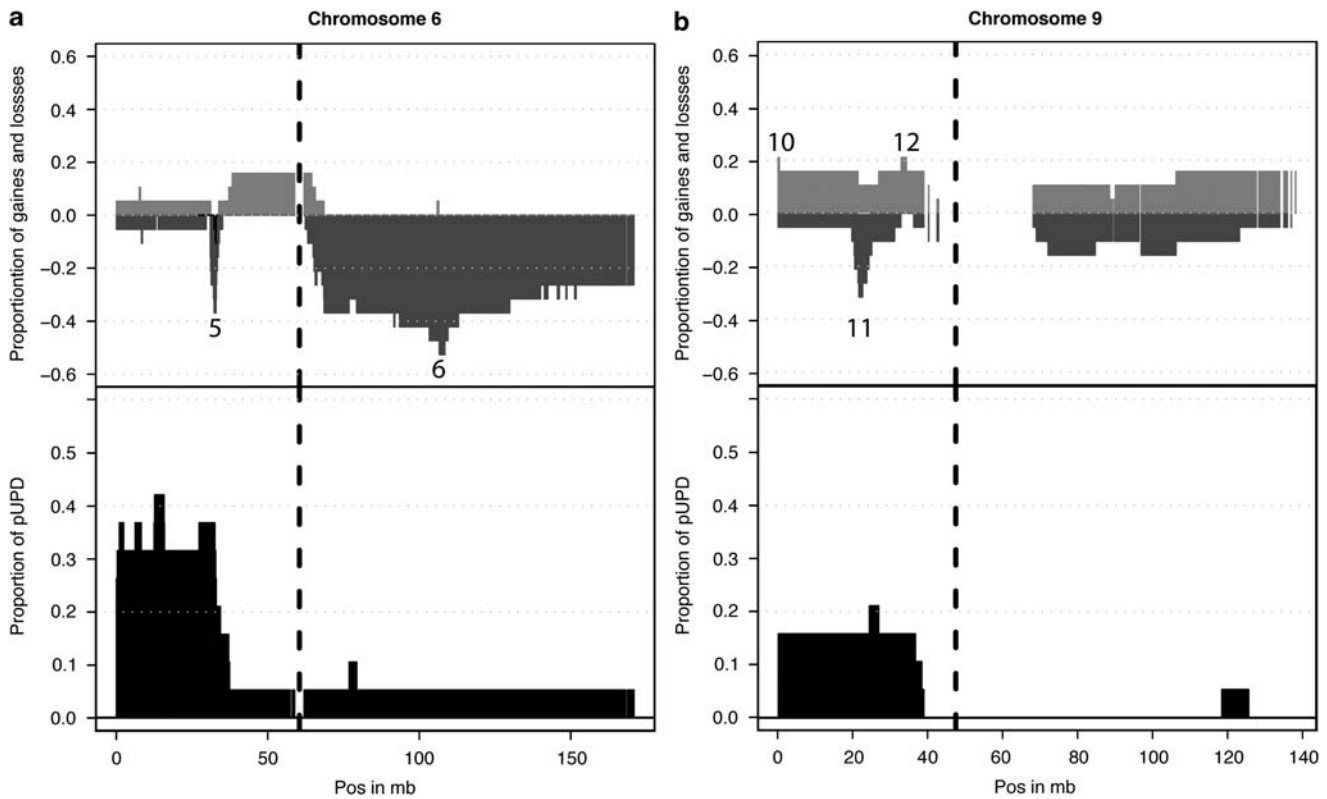


Figure 2 Imbalances and regions with pUPD at chromosome 6 (a) and chromosome 9 (b) analyzing 100k GeneChip data of 19 PCNSL. The chromosomes are displayed from pter (left) to qter (right). Proportion of deletions is indicated as dark gray columns and proportion of gains as light gray columns. Proportion of pUPD is separately displayed in black color. The numbers indicate MCR of frequent imbalances described in Table 2. 5: MCR of deletion in 6p21.32; 6: MCR of deletion in 6q21; 10: MCR of 9p24.3 (common CNV); 11: MCR of deletion in 9p21.3; and 12: MCR of gain in 9p13.3.

Gains were identified in 7q21.3–q22.1, 7q31.33, 9p24.3, 9p13.3, 12pter–qter, 14q11.2, 18q21.33–q23, 19q13.31, 19q13.43, and Xq21.33–q28. Genomic losses were frequently detected in 3p14.2, 4q12, 4q13.1, 4q35.2, 6p21.32, 6q21, 8q12.1–q12.2, 9p21.3, 10q23.21, 12p13.2 and 15q11.2. Some of these regions contain known CNVs, also present in healthy individuals (Table 2). The 100k GeneChip data of the PCNSL were also subjected to LOH analysis in order to detect regions of pUPD. Overall, we identified 78 regions of pUPD in 17 of these PCNSL with a median number of 4 pUPDs per PCNSL (range: 0–12). The genome-wide distribution of pUPD is shown in Figure 1b.

Loss of genetic material and pUPD

The region most commonly affected by loss or pUPD (14/19, 74%) was located in 6p21.32 (Figure 2a, Table 2, MCR 5). In two of these PCNSL (case nos. 04 and 05), homozygous loss was detected and subsequently confirmed by FISH. The MCR comprised 0.3 Mb and harbored the MHC class II encoding genes *HLA-DRB*, *HLA-DQA*, and *HLA-DQB*. Remarkably, the region most commonly affected by pUPD extended from the HLA region to the telomeric region of 6p.

Of the 19 PCNSL, 10 (53%) harbored a deletion in the long arm of chromosome 6 with an MCR of 2.0 Mb in 6q21 (Figure 2a, Table 2, MCR 6). The MCR encompassed 11 genes, among them the *PRDM1* gene. In this region, a pUPD was not detected. Sequencing of all exons of the *PRDM1* gene failed to detect any mutations of the second allele in the tumors with heterozygous deletion of *PRDM1*.

Six (32%) PCNSL carried a deletion in 8q12.1–q12.2 encompassing an MCR of 2.4 Mb, where *TOX*, *CA8* and *RAB2A* are located (Figure 3d, Table 2, MCR 9). In five of these cases, heterozygous deletion was confirmed by FISH. Six (32%) PCNSL showed a small (1.0 Mb) MCR of a deletion in 9p21.3 involving *CDKN2A/p16*, *CDKN2B/p15*, and *MTAP* (Figure 2b, Table 2, MCR 11). In one of these PCNSL, the deletion was homozygous. Further three PCNSL showed a pUPD in this region.

A small minimally deleted region affecting only one SNP within the 3p14.2 region was detected in 4 (21%) PCNSL, encompassing the *FHIT* gene locus (Figure 3a, Table 2, MCR 1). In 4 (21%) PCNSL, we detected a deletion of 0.4 Mb deletion in 4q12 involving the *SCFD2* gene locus (Figure 3b, Table 2, MCR 2). Another 0.8 Mb MCR of deletion was detected in 4q13.1 (Figure 3b, Table 2, MCR 3). In addition, 4 (21%) PCNSL showed a 1.5-Mb-sized MCR in 4q35.2, where the *FAT* gene is located (Figure 3b, Table 2, MCR 4). Two small (0.2 Mb) MCRs, one in 10q23.21 involving the *FAS* and *AMSH-LP* genes (Figure 3e, Table 2, MCR 13) and another in 12p13.2 affecting the *ETV6* gene (Figure 3f, Table 2, MCR 15), were observed in four (4/19, 21%) PCNSL. One PCNSL harboring a 12p13.2 deletion (PCNSL no. 13) even showed a homozygous loss, which was confirmed by FISH.

Gains of genetic material

Chromosomal gains affected regions ranging in size from 84 kb to whole chromosomes. Eight (43%) PCNSL showed a gain in 18q21.1–q23. In seven of these cases both *MALT1* and *BCL2*

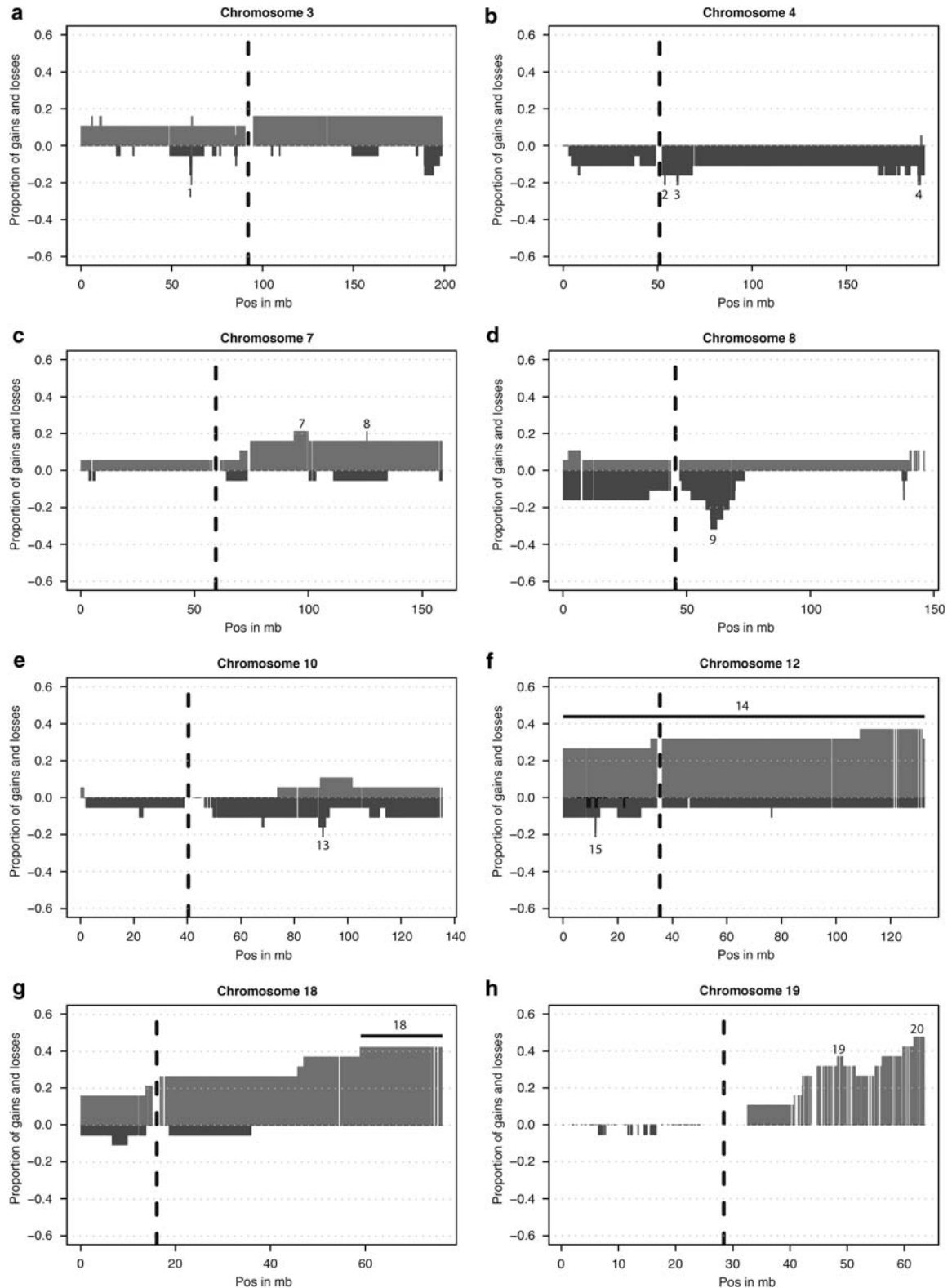


Figure 3 Detailed mapping of chromosomal imbalances in 19 PCNSL. Chromosomes 3 (a), 4 (b), 7 (c), 8 (d), 10 (e), 12 (f), 18 (g) and 19 (h) are displayed from pter (left) to qter (right). Proportions of deletions and gains are indicated as dark gray and light gray columns, respectively. The numbers indicate frequently altered MCR of frequent imbalances described in Table 2. 1: MCR of deletion in 3p14.2; 2: MCR of deletion in 4q12; 3: MCR of deletion in 4q13.1; 4: MCR of deletion in 4q35.2; 7: MCR of gain in 7q21.3–q22.1; 8: MCR in 7q31.33 (common CNV); 9: MCR of deletion in 8q12.1–q12.2; 13: MCR of deletion in 10q23.21; 14: gain of the entire chromosome 12; 15: MCR of deletion in 12p13.2; 18: MCR of gain in 18q21.33–q23; 19: MCR of gain in 19q13.31; and 20: MCR of gain in 19q13.43.

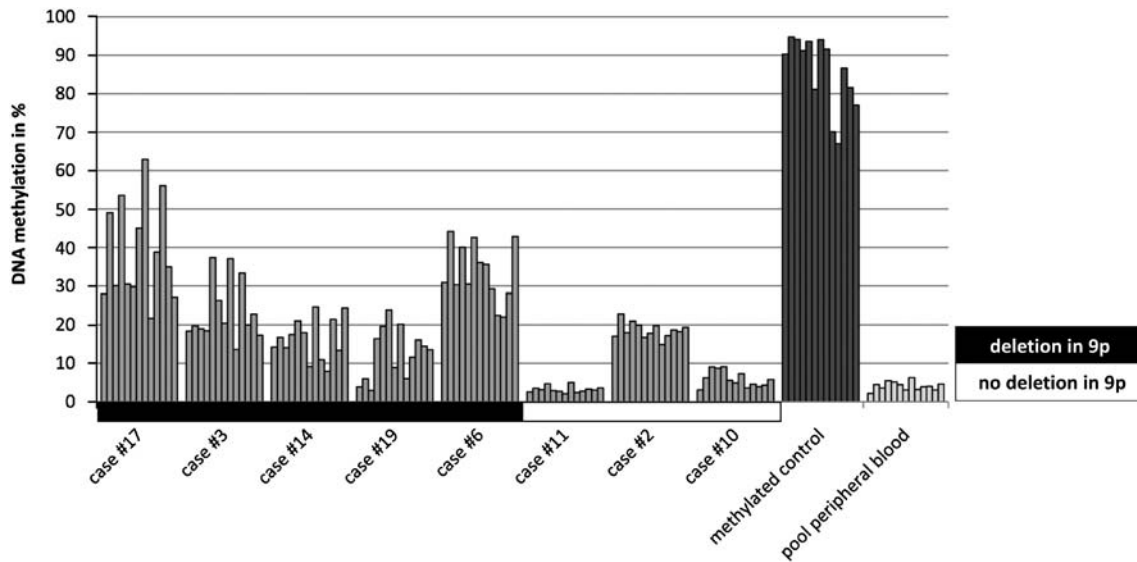


Figure 4 Pyrosequencing analysis of the *CDKN2A/p16* locus. Quantification of DNA methylation of 13 CpG dinucleotides within the promoter region of *CDKN2A/p16* by pyrosequencing. Methylation values of each CpG are shown as gray vertical bars for each analyzed sample. PCNSL are arranged according to their chromosomal aberrations in 9p affecting the *CDKN2A/p16* locus (black horizontal bar = heterozygous deletion in 9p, white horizontal bar = no deletion in 9p). PCNSL with 9p deletion showed higher methylation values compared to those without 9p deletion.

were affected, whereas in a single case only the *BCL2* gene was gained (Figure 3g, Table 2, MCR 18). These results were confirmed by FISH. Two small MCRs of chromosomal gain were detected in 19q13.31 (7/19, 37%, Figure 3h, MCR 19) and in 19q13.43 (9/19, 47%, Figure 3h, MCR 20). Both regions harbor several genes encoding zinc finger proteins. Five (26%) PCNSL showed a gain of the entire chromosome 12. In two additional cases, gain was restricted to bands 12p11.21–q24.33 and 12q24.11–q24.33, respectively (Figure 3f, MCR 14). Six (32%) PCNSL showed a gain of Xq21.33–q28 (MCR 21; whole chromosome X: 4/19, Table 2). Four of 19 (21%) PCNSL showed gains in 7q21.3–q22.1 (Figure 3c, MCR 7, Table 2). Four additional tumors harbored gains in 9p13.3 (Table 2), the latter containing the *NFX1* and *BAG1* genes (Figure 2b, MCR 12).

Comparison of MCR with gene expression profiles

To investigate the effect of chromosomal imbalances on expression of genes within the MCR, corresponding tags on the HG-U95Av2 platform were further studied (Table 2).²⁴ In 17 of 21 MCRs, at least one mRNA could be analyzed with respect to a differential expression between PCNSL with and without any alteration in the respective MCR. Only four MCRs showed a differential expression of at least one mRNA.

In MCR 13 (loss of 10q23.21), only one of seven mRNA was significantly differentially expressed ($P=1.9E-03$). As depicted in Supplementary Figure 1, *FAS* expression was very low in cases with alterations in this MCR but also in 5 of 14 PCNSL without alterations in MCR 13.

For MCR 14 (gain of chromosome 12), 668 tags were analyzed; of these, 203 of these tags were differentially expressed, whereas expression of 186 tags (92%) was below 100, that is, the defined background threshold. Seventeen tags, corresponding to 16 genes, were significantly differentially expressed at higher levels, including *STAT6* and *CD27* (Supplementary Figure 1).

In MCR 19 (gain of chromosome 19q13.31), one tag, corresponding to the gene *ETHE1*, was significantly differentially expressed ($P=9.8E-03$, Supplementary Figure 1).

In MCR 21 (gain of chromosome Xq21.33–q28), 87 of 217 tags showed a significantly differential expression. Expression values were below 100, that is, the defined background threshold, in 83 of 87 (95%) of these tags. The four tags with a differential expression corresponded to two genes, *ARHGGEF6* and *SEPT6* (Supplementary Figure 1).

Methylation status of the *CDKN2A/p16* locus in PCNSL

As shown in Figure 4, six of eight PCNSL showed increased methylation at the *CDKN2A/p16* locus compared with controls. Methylation in PCNSL with heterozygous deletion at the *CDKN2A/p16* locus was increased as compared with PCNSL without deletion in 9p, although this did not reach significance owing to the limited number of samples in each group. Thus, both deletions and DNA methylation may be considered as mechanisms of *CDKN2A/p16* inactivation in PCNSL.

Discussion

In this study, genomic imbalances and LOH were addressed in a series of 19 PCNSL using high-density oligonucleotide arrays. PCNSL showed multiple chromosomal imbalances. In addition to novel recurrent regions of genomic imbalances, unknown regions of pUPD were identified, and homozygous and heterozygous deletions in PCNSL involving the *HLA* locus and the tumor suppressor gene loci *MTAP*, *CDKN2A/p16*, and *CDKN2B/p15* were confirmed.

Alterations in 6p21.32 by deletion or pUPD were the most frequent abnormality (14/19, 73%). The altered region harbors the *HLA-DRB*, *HLA-DQA*, and *HLA-DQB* genes. These findings are in line with previous reports on homozygous and heterozygous deletions at the HLA class II locus, which were associated with a lack of MHC class II antigen expression by

the tumor cells of PCNSL. The progressive loss of MHC proteins may facilitate tumor cell escape from the immune response.^{11,12,28} This may be particularly relevant for lymphomas of immunoprivileged organs such as brain and testis, which are characterized by a physiologically downregulated immunophenotype, including low numbers of lymphocytes. In fact, in extracerebral DLBCL, decreased CD8 T-cell numbers have been noticed in MHC class II-negative as compared with MHC class II-positive tumors (median: 2.8 vs 11%), and MHC class II-negative DLBCL were correlated with a poor outcome.^{29,30}

Ten (53%) PCNSL showed a deletion involving 6q21, being in accordance with data reported previously.^{7,10} The chromosomal region 6q21 is frequently deleted in various B-cell malignancies, including DLBCL, mantle cell lymphoma, acute lymphatic leukemia and immunoblastic lymphoma.^{7,31–35} This region has been suggested to harbor a tumor suppressor gene. In fact, 6q21 contains the *PRDM1* gene encoding BLIMP1, which has recently been reported to function as tumor suppressor gene in PCNSL as well as in systemic DLBCL of the activated B-cell type.^{25,34,36} In a significant fraction (4/21, 21%) of PCNSL, inactivating mutations of the *PRDM1* gene were associated with loss of BLIMP1 protein expression.²⁵ These mutations may contribute to tumorigenesis by blocking terminal B-cell differentiation. In this context, it is of note that the tumor cells of PCNSL are impaired in their differentiation as they do not perform Ig class switch recombination and, thus, are characterized by an IgM+IgD+ phenotype.³⁷ However, in this study, sequencing analysis of 8 of the 10 identified PCNSL with 6q21 deletion failed to detect any *PRDM1* mutation, which could suggest that either biallelic *BLIMP1* inactivation is a secondary event in PCNSL or that alternative means of *BLIMP1* inactivation exist in PCNSL.

SNP chip analysis also showed heterozygous deletions in 8q with a 2.4-Mb MCR between 8q12.1 and 8q12.2 in 6 of 19 (32%) PCNSL. This MCR harbors a gene encoding the nuclear factor *TOX* (*KIAA0808*), which is required for CD4 T-cell development.³⁸ Is it interesting that the IgG+ B-cell population was reduced in the spleen of *TOX*-deficient mice. However, early steps of B-cell development apparently were normal in these animals. It is intriguing to speculate that *TOX* may contribute to the observed arrest of B-cell differentiation in PCNSL. *TOX* has been reported to be also deleted in 4% (8/205) of childhood acute lymphatic leukemia.³⁹ Further candidate genes within the 8q12.1–8q12.2 region are the potential oncogene *CA8*, which promotes growth, proliferation and invasion of carcinoma cells,^{40–42} and the *RAB2A* gene encoding the ras-related rab2.

The tumor suppressor genes, *CDKN2A/p16* and *CDKN2B/p15*, at 9p21.3 as well as *MTAP* were targeted by recurrent deletions and pUPD present in 6 and 3 of 19 (32 and 16%) PCNSL, respectively. One PCNSL even showed a biallelic loss.⁴³ Furthermore, *CDKN2A/p16* has been shown to be methylated in 64% (16/25) in PCNSL.⁴⁴ P16, that is, one of the encoded proteins, specifically inhibits CDK4 and CDK6 and potentially blocks G1 cell-cycle progression through the dephosphorylation of retinoblastoma through its inhibitory effect on the CDK4/cyclin D1 complex activity.⁴⁵ Compared with previous studies, in which DNA methylation of the *CDKN2A/p16* locus in PCNSL was mostly analyzed by methylation-specific PCR, we accurately quantitated methylation of 13 CpG dinucleotides by bisulfite pyrosequencing of DNA from eight PCNSL of this series. Our identification of recurrent *CDKN2A/p16* promoter methylation, which likely leads to its inactivation, is in accordance with Chu *et al.*⁴⁴ Moreover, the frequent

methylation of the gene in PCNSL with heterozygous deletions suggests that biallelic inactivation in these tumors may result from two different mechanisms, that is DNA methylation and chromosomal deletion.

Additional recurrent deletions present in at least 4 (21%) PCNSL were in 3p14.2, 4q12, 4q13.1, 4q35.2, 10q23.21, and 12p13.2. In 3p14.2, the *FHIT* gene was partially deleted. *FHIT*, which is supposed to have a key function in tumor suppression,^{46,47} has been shown to be either deleted or mutated in 33% (19/57) of systemic DLBCL. Clinically relevant, decreased *FHIT* expression has been reported to correlate with an inferior prognosis in systemic DLBCLs.⁴⁸ In 4q12, a 200-kb MCR of deletion involving the *SCFD2* gene, a potential p53 target gene, was detected.⁴⁹ In 4q35.2, the *FAT* tumor suppressor gene was affected by deletion. Another small MCR of deletion affected the tumor suppressor gene *FAS* gene at 10q23.21. *FAS* (CD95), a transmembrane receptor of the tumor necrosis factor superfamily, is an important mediator of apoptosis.⁵⁰ *FAS* mutations, which may impair apoptosis, have been identified in 20% (2/10) PCNSL.¹⁵ In 12p13.2, a 200-kb MCR of deletion was detected with one PCNSL showing biallelic loss; in another PCNSL, the pattern of imbalances suggested a deletion to have occurred before amplification of an allele. The deletions affected the *ETV6* gene, which is frequently translocated in hematopoietic tumors.⁵¹

In PCNSL, recurrent gains in 18q have been described by various groups.^{1,5–7,10} 18q21 harbors the *BCL2* and *MALT1* genes. *MALT1* complexes with *BCL10* and a *CARD* protein to activate the nuclear factor- κ B pathway.⁵² In fact, both *MALT1* and *BCL10* are expressed by the tumor cells of PCNSL, which also show evidence for an activation of the nuclear factor- κ B pathway.⁵³ In our study, 8/19 PCNSL and 7/19 PCNSL showed gains of *BCL2* and *MALT1*, respectively. Microarray data identified two small MCRs frequently gained in 19q13.31 and 19q13.43. Both regions harbor several genes encoding zinc finger proteins, which might be involved in transcriptional regulation. This region partly overlaps with a region of gain in 19q13.12–13.43 detected in 2 (22%) PCNSL recently.¹⁰ In accordance with previous observations,^{5–7} two PCNSL showed gains of 12p11.21–q24.33 and 12q24.11–12q24.33, and five further tumors showed triploidy of chromosome 12. Furthermore, PCNSL had two small MCRs of copy number gains in 7q21.3–q22.1 and 9p21.1–p21.3 and one large MCR of recurrent copy number gain in Xq21.33–q28. The region 7q21.3–q22.1 harbors the candidate genes *NFX1* and *BAG1*. *NFX1* is a nuclear transcription factor, which downregulates HLA class II antigen expression.⁵⁴ *Bag1* interacts with *Bcl2* to increase its antiapoptotic activity.⁵⁵

It is tempting to speculate that PCNSL corresponding to the ABC and GCB subgroups as defined for systemic^{56–58} may be characterized by different patterns of genomic aberrations indicating particular and distinct pathways relevant for pathogenesis. In this series of PCNSL, MCR 2 (loss 4q12), MCR 3 (loss 4q13.1), and MCR 15 (loss 12p13.2) were exclusively associated with the ABC-type, whereas MCR 14 (gain chromosome 12) was only observed in the GCB-subtype of PCNSL. However, this observation should be interpreted with caution due to the low number of PCNSL available for such studies, which precludes such an analysis.

In conclusion, the identification of novel candidate tumor suppressor genes and oncogene loci through high-density oligonucleotide SNP array analysis may provide the basis for further studies aiming at the identification of genes involved in PCNSL tumorigenesis.

Conflict of Interest

The authors declare no conflict of interest.

Acknowledgements

This study was supported by the Deutsche Krebshilfe/Dr Mildred Scheel Stiftung für Krebsforschung (Grant no. 107733). The Affymetrix and pyrosequencing platforms were provided by the KinderKrebsInitiative Buchholz/Holm-Seppensen.

References

- Montesinos-Rongen M, Siebert R, Deckert M. Primary lymphoma of the central nervous system: just DLBCL or not? *Blood* 2009; **113**: 7–10.
- Schlegel U, Schmidt-Wolf IG, Deckert M. Primary CNS lymphoma: clinical presentation, pathological classification, molecular pathogenesis and treatment. *J Neurol Sci* 2000; **181**: 1–12.
- Deckert M, Paulus W. Malignant lymphomas. In: Louis DN, Ohgaki H, Wiestler OD, Cavenee WK (eds). *WHO Classification of Tumors Pathology and Genetics of Tumours of the Nervous System*, 4th edn. IRAC: Lyon, 2007, pp. 188–192.
- Kluin P, Deckert M, Ferry JA. Primary diffuse large B-cell lymphoma of the CNS. In: Swerdlow SH, Campo E, Harris NL, Jaffe ES, Pileri SA, Stein H, et al. (eds). *WHO Classification of Tumours of Haematopoietic and Lymphoid Tissues*. IARC: Lyon, 2008, pp. 240–241.
- Montesinos-Rongen M, Zühlke-Jenisch R, Gesk S, Martin-Subero JI, Schaller C, Van Roost D et al. Interphase cytogenetic analysis of lymphoma-associated chromosomal breakpoints in primary diffuse large B-cell lymphomas of the central nervous system. *J Neuropathol Exp Neurol* 2002; **61** (10): 926–933.
- Rickert CH, Dockhorn-Dworniczak B, Simon R, Paulus W. Chromosomal imbalances in primary lymphomas of the central nervous system. *Am J Pathol* 1999; **155**: 1445–1451.
- Weber T, Weber RG, Kaulich K, Actor B, Meyer-Puttlitz B, Lampel S et al. Characteristic chromosomal imbalances in primary central nervous system lymphomas of the diffuse large B-cell type. *Brain Pathol* 2000; **10**: 73–84.
- Montesinos-Rongen M, Akasaka T, Zühlke-Jenisch R, Schaller C, Van Roost D, Wiestler OD et al. Molecular characterization of BCL6 breakpoints in primary diffuse large B-cell lymphomas of the central nervous system identifies GAPD as novel translocation partner. *Brain Pathol* 2003; **13**: 534–538.
- Schwindt H, Akasaka T, Zühlke-Jenisch R, Hans V, Schaller C, Klapper W et al. Chromosomal translocations fusing the BCL6 gene to different partner loci are recurrent in primary central nervous system lymphoma and may be associated with aberrant somatic hypermutation or defective class switch recombination. *J Neuropathol Exp Neurol* 2006; **65**: 776–782.
- Booman M, Szuhai K, Rosenwald A, Hartmann E, Kluin-Nelemans H, de Jong D et al. Genomic alterations and gene expression in primary diffuse large B-cell lymphomas of immune-privileged sites: the importance of apoptosis and immunomodulatory pathways. *J Pathol* 2008; **216**: 209–217.
- Jordanova ES, Riemersma SA, Philippo K, Giphart-Gassler M, Schuurin E, Kluin PM. Hemizygous deletions in the HLA region account for loss of heterozygosity in the majority of diffuse large B-cell lymphomas of the testis and the central nervous system. *Genes Chromosomes Cancer* 2002; **35**: 38–48.
- Riemersma SA, Jordanova ES, Schop RF, Philippo K, Looijenga LH, Schuurin E et al. Extensive genetic alterations of the HLA region, including homozygous deletions of HLA class II genes in B-cell lymphomas arising in immune-privileged sites. *Blood* 2000; **96**: 3569–3577.
- Brunn A, Montesinos-Rongen M, Strack A, Reifenberger G, Mawrin C, Schaller C et al. Expression pattern and cellular sources of chemokines in primary central nervous system lymphoma. *Acta Neuropathol (Berl)* 2007; **114**: 271–276.
- Montesinos-Rongen M, Küppers R, Schlüter D, Spieker T, Van Roost D, Schaller C et al. Primary central nervous system lymphomas are derived from germinal-center B cells and show a preferential usage of the V4–34 gene segment. *Am J Pathol* 1999; **155**: 2077–2086.
- Montesinos-Rongen M, Van Roost D, Schaller C, Wiestler OD, Deckert M. Primary diffuse large B-cell lymphomas of the central nervous system are targeted by aberrant somatic hypermutation. *Blood* 2004; **103**: 1869–1875.
- Kennedy GC, Matsuzaki H, Dong S, Liu WM, Huang J, Liu G et al. Large-scale genotyping of complex DNA. *Nat Biotechnol* 2003; **21**: 1233–1237.
- Affymetrix. BRLMM: an improved genotype calling method for the GeneChip human mapping 500k array set. 2006, White Paper: Affymetrix Inc.
- Nannya Y, Sanada M, Nakazaki K, Hosoya N, Wang L, Hangaishi A et al. A robust algorithm for copy number detection using high-density oligonucleotide single nucleotide polymorphism genotyping arrays. *Cancer Res* 2005; **65**: 6071–6079.
- lafrate AJ, Feuk L, Rivera MN, Listewnik ML, Donahoe PK, Qi Y et al. Detection of large-scale variation in the human genome. *Nat Genet* 2004; **36**: 949–951.
- Beroukhim R, Lin M, Park Y, Hao K, Zhao X, Garraway LA et al. Inferring loss-of-heterozygosity from unpaired tumors using high-density oligonucleotide SNP arrays. *PLoS Comput Biol* 2006; **2**: e41.
- Lin M, Wei LJ, Sellers WR, Lieberfarb M, Wong WH, Li C. dChipSNP: significance curve and clustering of SNP-array-based loss-of-heterozygosity data. *Bioinformatics* 2004; **20**: 1233–1240.
- Zhao X, Li C, Paez JG, Chin K, Janne PA, Chen TH et al. An integrated view of copy number and allelic alterations in the cancer genome using single nucleotide polymorphism arrays. *Cancer Res* 2004; **64**: 3060–3071.
- Barrett T, Troup DB, Wilhite SE, Ledoux P, Rudnev D, Evangelista C et al. NCBI GEO: mining tens of millions of expression profiles—database and tools update. *Nucleic Acids Res* 2007; **35**: D760–D765.
- Montesinos-Rongen M, Brunn A, Bentink S, Basso K, Lim WK, Klapper W et al. Gene expression profiling suggests primary central nervous system lymphomas to be derived from a late germinal center B cell. *Leukemia* 2008; **22**: 400–405.
- Courts C, Montesinos-Rongen M, Brunn A, Bug S, Siemer D, Hans V et al. Recurrent inactivation of the PRDM1 gene in primary central nervous system lymphoma. *J Neuropathol Exp Neurol* 2008; **67**: 720–727.
- Martin-Subero JI, Harder L, Gesk S, Schlegelberger B, Grote W, Martinez-Climent JA et al. Interphase FISH assays for the detection of translocations with breakpoints in immunoglobulin light chain loci. *Int J Cancer* 2002; **98**: 470–474.
- Tost J, Gut IG. Analysis of gene-specific DNA methylation patterns by pyrosequencing technology. *Methods Mol Biol* 2007; **373**: 89–102.
- Booman M, Douwes J, Glas AM, Riemersma SA, Jordanova ES, Kok K et al. Mechanisms and effects of loss of human leukocyte antigen class II expression in immune-privileged site-associated B-cell lymphoma. *Clin Cancer Res* 2006; **12**: 2698–2705.
- List AF, Spier CM, Miller TP, Grogan TM. Deficient tumor-infiltrating T-lymphocyte response in malignant lymphoma: relationship to HLA expression and host immunocompetence. *Leukemia* 1993; **7**: 398–403.
- Rimsza LM, Roberts RA, Miller TP, Unger JM, LeBlanc M, Brazier RM et al. Loss of MHC class II gene and protein expression in diffuse large B-cell lymphoma is related to decreased tumor immunosurveillance and poor patient survival regardless of other prognostic factors: a follow-up study from the Leukemia and Lymphoma Molecular Profiling Project. *Blood* 2004; **103**: 4251–4258.
- Boonstra R, Koning A, Mastik M, van den Berg A, Poppema S. Analysis of chromosomal copy number changes and oncoprotein expression in primary central nervous system lymphomas: frequent loss of chromosome arm 6q. *Virchows Arch* 2003; **443**: 164–169.
- Bosga-Bouwer AG, Kok K, Booman M, Boven L, van der Vlies P, van den Berg A et al. Array comparative genomic hybridization reveals a very high frequency of deletions of the long arm of chromosome 6 in testicular lymphoma. *Genes Chromosomes Cancer* 2006; **45**: 976–981.
- Bosga-Bouwer AG, van den Berg A, Haralambieva E, de Jong D, Boonstra R, Kluin P et al. Molecular, cytogenetic, and immuno-

- phenotypic characterization of follicular lymphoma grade 3B; a separate entity or part of the spectrum of diffuse large B-cell lymphoma or follicular lymphoma? *Hum Pathol* 2006; **37**: 528–533.
- 34 Pasqualucci L, Compagno M, Houldsworth J, Monti S, Grunn A, Nandula SV *et al.* Inactivation of the PRDM1/BLIMP1 gene in diffuse large B cell lymphoma. *J Exp Med* 2006; **203**: 311–317.
 - 35 Thelander EF, Ichimura K, Corcoran M, Barbany G, Nordgren A, Heyman M *et al.* Characterization of 6q deletions in mature B cell lymphomas and childhood acute lymphoblastic leukemia. *Leuk Lymphoma* 2008; **49**: 477–487.
 - 36 Tam W, Gomez M, Chadburn A, Lee JW, Chan WC, Knowles DM. Mutational analysis of PRDM1 indicates a tumor-suppressor role in diffuse large B-cell lymphomas. *Blood* 2006; **107**: 4090–4100.
 - 37 Montesinos-Rongen M, Schmitz R, Courts C, Stenzel W, Bechtel D, Niedobitek G *et al.* Absence of immunoglobulin class switch in primary lymphomas of the central nervous system. *Am J Pathol* 2005; **166**: 1773–1779.
 - 38 Aliahmad P, Kaye J. Development of all CD4T lineages requires nuclear factor TOX. *J Exp Med* 2008; **205**: 245–256.
 - 39 Bardet V, Couque N, Cattolico L, Hetet G, Devaux I, Duprat S *et al.* Molecular analysis of nonrandom 8q12 deletions in acute lymphoblastic leukemia: identification of two candidate genes. *Genes Chromosomes Cancer* 2002; **33**: 178–187.
 - 40 Lu SH, Takeuchi T, Fujita J, Ishida T, Akisawa Y, Nishimori I *et al.* Effect of carbonic anhydrase-related protein VIII expression on lung adenocarcinoma cell growth. *Lung Cancer* 2004; **44**: 273–280.
 - 41 Morimoto K, Nishimori I, Takeuchi T, Kohsaki T, Okamoto N, Taguchi T *et al.* Overexpression of carbonic anhydrase-related protein XI promotes proliferation and invasion of gastrointestinal stromal tumors. *Virchows Arch* 2005; **447**: 66–73.
 - 42 Nishikata M, Nishimori I, Taniuchi K, Takeuchi T, Minakuchi T, Kohsaki T *et al.* Carbonic anhydrase-related protein VIII promotes colon cancer cell growth. *Mol Carcinog* 2007; **46**: 208–214.
 - 43 Haller F, Lobke C, Ruschhaupt M, Cameron S, Schulten HJ, Schwager S *et al.* Loss of 9p leads to p16INK4A down-regulation and enables RB/E2F1-dependent cell cycle promotion in gastrointestinal stromal tumours (GISTs). *J Pathol* 2008; **215**: 253–262.
 - 44 Chu LC, Eberhart CG, Grossman SA, Herman JG. Epigenetic silencing of multiple genes in primary CNS lymphoma. *Int J Cancer* 2006; **119**: 2487–2491.
 - 45 Serrano M, Hannon GJ, Beach D. A new regulatory motif in cell-cycle control causing specific inhibition of cyclin D/CDK4. *Nature* 1993; **366**: 704–707.
 - 46 Fujishita T, Doi Y, Sonoshita M, Hiai H, Oshima M, Huebner K *et al.* Development of spontaneous tumours and intestinal lesions in Fhit gene knockout mice. *Br J Cancer* 2004; **91**: 1571–1574.
 - 47 Kameoka Y, Tagawa H, Tsuzuki S, Karnan S, Ota A, Suguro M *et al.* Contig array CGH at 3p14.2 points to the FRA3B/FHIT common fragile region as the target gene in diffuse large B-cell lymphoma. *Oncogene* 2004; **23**: 9148–9154.
 - 48 Chen PM, Yang MH, Hsiao LT, Yu IT, Chu CJ, Chao TC *et al.* Decreased FHIT protein expression correlates with a worse prognosis in patients with diffuse large B-cell lymphoma. *Oncol Rep* 2004; **11**: 349–356.
 - 49 Krieg AJ, Hammond EM, Giaccia AJ. Functional analysis of p53 binding under differential stresses. *Mol Cell Biol* 2006; **26**: 7030–7045.
 - 50 Oehm A, Behrmann I, Falk W, Pawlita M, Maier G, Klas C *et al.* Purification and molecular cloning of the APO-1 cell surface antigen, a member of the tumor necrosis factor/nerve growth factor receptor superfamily. Sequence identity with the Fas antigen. *J Biol Chem* 1992; **267**: 10709–10715.
 - 51 Wlodarska I, Mecucci C, Baens M, Marynen P, van den Berghe H. ETV6 gene rearrangements in hematopoietic malignant disorders. *Leuk Lymphoma* 1996; **23**: 287–295.
 - 52 Ferch U, zum Buschenfelde CM, Gewies A, Wegener E, Rauser S, Peschel C *et al.* MALT1 directs B cell receptor-induced canonical nuclear factor-kappaB signaling selectively to the c-Rel subunit. *Nat Immunol* 2007; **8**: 984–991.
 - 53 Courts C, Montesinos-Rongen M, Martin-Subero JL, Brunn A, Siemer D, Zühlke-Jenisch R *et al.* Transcriptional profiling of the nuclear factor-kappaB pathway identifies a subgroup of primary lymphoma of the central nervous system with low BCL10 expression. *J Neuropathol Exp Neurol* 2007; **66**: 230–237.
 - 54 Song Z, Krishna S, Thanos D, Strominger JL, Ono SJ. A novel cysteine-rich sequence-specific DNA-binding protein interacts with the conserved X-box motif of the human major histocompatibility complex class II genes via a repeated Cys–His domain and functions as a transcriptional repressor. *J Exp Med* 1994; **180**: 1763–1774.
 - 55 Takayama S, Sato T, Krajewski S, Kochel K, Irie S, Millan JA *et al.* Cloning and functional analysis of BAG-1: a novel Bcl-2-binding protein with anti-cell death activity. *Cell* 1995; **80**: 279–284.
 - 56 Alizadeh AA, Eisen MB, Davis RE, Ma C, Lossos IS, Rosenwald A *et al.* Distinct types of diffuse large B-cell lymphoma identified by gene expression profiling. *Nature* 2000; **403**: 503–511.
 - 57 Lenz G, Wright GW, Emre NC, Kohlhammer H, Dave SS, Davis RE *et al.* Molecular subtypes of diffuse large B-cell lymphoma arise by distinct genetic pathways. *Proc Natl Acad Sci USA* 2008; **105**: 13520–13525.
 - 58 Rosenwald A, Wright G, Chan WC, Connors JM, Campo E, Fisher RI *et al.* The use of molecular profiling to predict survival after chemotherapy for diffuse large-B-cell lymphoma. *N Engl J Med* 2002; **346**: 1937–1947.

Supplementary Information accompanies the paper on the Leukemia website (<http://www.nature.com/leu>)